Spectrochimica Acta Part A: Molecular and Biomolecular Spectroscopy 323 (2024) 124903

Contents lists available at ScienceDirect

Spectrochimica Acta Part A:
Molecular and Biomolecular Spectroscopy

journal homepage: www.journals.elsevier.com/spectrochimica-acta-part-a-molecular-and-biomolecular-spectroscopy

Raman spectroscopy as a tool for characterisation of quality parameters in Norwegian grown apples during ripening

Olga Monago-Maraña [a,b,*], Jens Petter Wold [b], Siv Fagertun Remberg [c], Karen Wahlstrøm Sanden [b], Nils Kristian Afseth [b]

[a] Department of Analytical Sciences, Faculty of Science, Universidad Nacional de Educación a Distancia (UNED), Avda. Esparta s/n, Crta. de Las Rozas-Madrid, 28232, Las Rozas, Madrid, Spain
[b] Nofima AS – Norwegian Institute of Food, Fisheries and Aquaculture Research, Muninbakken 9-13, Breivika, Postboks 6122 Langnes, NO-9291 Tromsø, Norway
[c] Faculty of Biosciences, Department of Plant Sciences, Norwegian University of Life Sciences, PO-BOX 5003, 1432 Ås, Norway

HIGHLIGHTS

- The ripening process of apple fruits was followed using Raman spectroscopy.
- Non-destructive determination of starch index was performed by Raman spectroscopy.
- Raman spectra expressed distinct vibrational bands for starch and sugars.
- Raman is a potential future tool in harvest management of apples.

GRAPHICAL ABSTRACT

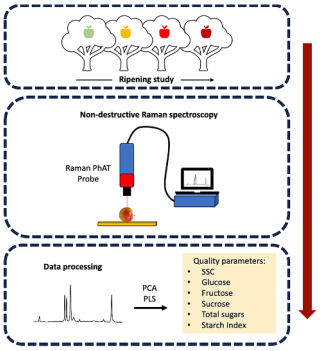

ARTICLE INFO

Keywords:
Starch index
Soluble solids content
Fructose
Glucose
Sucrose
Raman spectroscopy

ABSTRACT

This study shows for the first time the feasibility of Raman spectroscopy as a non-destructive method to follow the ripening process of apple fruits. Two different varieties of apples were studied: 'Aroma' and 'Elstar'. By visual inspection, Raman spectra showed that the starch content was higher in 'Elstar' apples compared to 'Aroma'. The degradation of starch over time could be detected in the Raman spectra, indicating that the method can be used to monitor the ripening process. The ripeness markers starch index, soluble solids content (SSC), and the sugars glucose, fructose and sucrose were determined with traditional destructive methods. Cross validated calibration models based on Raman spectroscopy were obtained for all quality parameters, and test set validation offered good results, with R^2 in the range 0.4–0.86 for 'Aroma' and 0.4–0.95 for 'Elstar', respectively. The regression coefficients showed that the calibrations relied on Raman bands associated with starch and different sugars. The

* Corresponding author.
E-mail address: olgamonago@ccia.uned.es (O. Monago-Maraña).

https://doi.org/10.1016/j.saa.2024.124903
Received 20 March 2024; Received in revised form 12 July 2024; Accepted 28 July 2024
Available online 30 July 2024
1386-1425/© 2024 The Author(s). Published by Elsevier B.V. This is an open access article under the CC BY-NC-ND license (http://creativecommons.org/licenses/by-nc-nd/4.0/).

results suggest that Raman spectroscopy in the future could be used to determine the optimal time of harvesting and to sort apples into different degrees of ripeness.

1. Introduction

As the development of autonomous harvesting systems for automated fruit picking and post-harvest sorting continues, there is an increasing need for portable and non-destructive tools for detailed characterization of fruit composition [1]. For apples, this is not least related to determining the optimal harvesting time, which significantly affects storage time and post-harvest quality attributes. Premature picking affects both taste and the probability of development of storage disorders, whereas fruits picked after optimal harvesting time can develop unwanted physical properties (e.g., mealiness) as well as physiological disorders, e.g. internal breakdown [2]. Common chemical attributes for monitoring the maturation process include starch and sugar contents [2]. Moreover, for determining overall consumer acceptability, sensory properties such as sweetness are important [3]. Sweetness has been shown to correlate well with soluble solid content (SSC) which includes organic acids, amino acids, soluble pectins and sugars (i.e., fructose, sucrose, and glucose) [4]. Whereas refractometry of apple juice is the standard destructive method for SSC measurement, near-infrared spectroscopy (NIRS) is an established alternative non-destructive technique. In addition, NIRS has been used for determination of starch content during apple ripening stages to ensure good quality properties [5,6], however only a few studies have reported promising results with NIRS for determining starch index [7,8]. NIRS sensors for use in sorting lines are commercially available [9], but challenges with NIRS sensors include lack of specificity on chemical properties and the need for extensive calibration to ensure robust results in different fruit varieties and from season to season [9].

Raman spectroscopy is a rapid and non-destructive technique that relies on inelastic scattering of photons (Raman scattering). The technique belongs to the family of vibrational spectroscopy, along with, for instance, NIRS. Due to its mechanism of action, Raman spectroscopy potentially offers more detailed insights at the molecular level compared to NIRS [10]. The technique is therefore also increasingly used within food analysis [11]. Raman spectra contain detailed information that can be used to identify carbohydrates such as glucose, fructose and sucrose, and for the characterization of starch [12]. Mono- and disaccharides provide a variety of distinct spectral features from around 1500 cm^{-1} and down into the fingerprinting region, with the ring deformation mode as one of the most dominating bands [12]. The technique is therefore frequently used for quantitative analysis in more complex samples. Özbalci et al. could for instance quantify sucrose, glucose, fructose, and maltose in diluted honey samples with high predictive performance using a Raman system with 785 nm laser excitation [13]. Similarly, Ilaslan et al. used Raman spectroscopy for quantification of glucose, sucrose and fructose in commercial soft drinks, also with high predictive performance [14]. Moreover, Raman spectroscopy has been extensively studied for the characterization and quantification of starch. For instance, Almeida et al. used FT-Raman spectroscopic analysis of native starches of different origin to quantify amylose content [15] with high predictive performance. Ji et al. also showed that quantification of starch in live, unicellular microalgae is possible using Raman spectroscopy [16]. All in all, this shows some of the potential of using Raman spectroscopy for detailed characterization of carbohydrates.

A prerequisite in food analysis is representative sampling of sometimes rather heterogeneous food matrices. In recent years, we have seen the development of sampling approaches enabling improved Raman sampling and also deeper optical probing in biological tissues [17]. One example is spatially offset Raman spectroscopy (SORS) [18], a technique that in the food area have particularly been used to characterize internal food qualities like maturation stages and optimal harvesting times of tomatoes [19,20]. Another example is wide area illumination Raman probes, employing an unfocused or loosely focused laser, increasing both the penetration depth and area of illumination of the laser spot [17]. Recently such probes have been used for characterization of a variety of food matrices, from poultry [21] and pork [22] to seafood [23], also paving the way for future in-line food analysis [24,25]. Andersen et al. used this approach for analysis of sugars and acids in whole strawberries [26]. Here, both individual sugars and total acids could be predicted with high predictive performances. It should be noted, however, that individual sugars were highly correlated to total sugars, meaning that these parameters could not be modelled independently. Recently, we also used wide area illumination Raman spectroscopy to study the potential for quantification of soluble solids and individual sugars in apples [27]. In this study, both intact apples and apples without skin were used, where the results indicated that Raman signals could penetrate to a depth of approximately 8 mm into an apple [27]. The results also showed that SSC, glucose and sucrose could be predicted with a good predictive performance in peeled apples.

The above-mentioned apple study was a feasibility study where a total of 60 apples from 6 varieties were randomly picked from boxes at a grocery store and subsequently analyzed. The apples were fully matured and consequently had negligible starch contents. The main objective of the present work was to use Raman spectroscopy to evaluate different quality parameters in two late apple varieties 'Aroma' and 'Elstar' to investigate if it is possible to measure and monitor the starch index and individual sugars. Apples were picked over of a period of approximately 1 month, and a total of 195 apple samples were subjected to Raman and reference analysis (i.e., individual sugars, SSC, and starch index). Raman analyses were performed on both intact and peeled apples, and to the authors knowledge, this is the first time Raman spectroscopy is used on whole intact apples to follow their changes in starch index and sugars through ripening process.

2. Materials and methods

2.1. Samples and chemicals

In this study, two sample sets were collected with apples harvested at the Norwegian University of Life Sciences at Ås, Norway (59°40′ N, 10°45′ E). The first set consisted of 105 'Aroma' apples. The apples were harvested at 7 different days over 4 weeks and measurements were conducted at the day of harvest. Harvest dates are shown in Table 1. The second sample set consisted of 90 'Elstar' apples. Samples were harvested at 6 days over 3 weeks and measurements were done at the same day of harvest. Harvest dates are shown in Table 1.

Standards for individual sugars (glucose, fructose, and sucrose) were obtained from Merck (Oslo, Norway). Trehalose (used as internal

Table 1
Date of fruit harvest (in year 2020) with number of samples per date and total.

Cv. Aroma		Cv. Elstar	
Date of harvest	**Number of samples**	**Date of harvest**	**Number of samples**
18th September	15	6th October	15
21st September	15	9th October	15
24th September	15	12th October	15
28th September	15	15th October	15
1st October	15	19th October	15
5th October	15	22nd October	15
8th October	15		
Total	**105**	**Total**	**90**

standard) was provided from VWR Life Science (Oslo, Norway). The reagents used for mobile phase (sodium acetate and sodium hydroxide solution (50 – 52 % in water)) were bought from Merck (Oslo, Norway).

Iodine was acquired from VWR, and potassium iodide was obtained from Merck (Oslo, Norway). A Milli-Q water system (Merck, Oslo, Norway) was used to obtain pure water.

2.2. Reference analyses

Different reference analyses were performed to evaluate the ripening of apples and for calibration with the Raman spectroscopy. A RE40 digital refractometer (Mettler Toledo AS, Oslo) was used for soluble solids content (SSC), expressed in percentage. All measurements were obtained from fresh juice samples, produced after peeling and removing the peduncle, with a juice maker. Juices were then frozen for further analysis of glucose, fructose, and sucrose, determined by liquid chromatography.

The chromatography analysis was performed in a diluted aliquot of juice (1:2000) with Milli-Q water containing 10 μg/mL of trehalose as internal standard in each sample. The method is thoroughly described by Helgerud et al. [28], and was used in a previous study by Monago et al. [27].

Starch index was determined using a visual method consisting of cutting the apple in half and introducing the apple in an iodine solution [29]. After that, an index from 1 (high starch content) to 10 (low starch content) is given by a visual inspection and comparison with a scale [30]. The iodine solution was prepared in a 1000 mL volumetric flask, adding 10 g of potassium iodine and 2 g of iodide solution. Previously, each reagent was dissolved in 100 mL of distilled water.

2.3. Raman spectroscopy

Raman spectra were collected with a RamanRXN2™ Hybrid system (Kaiser Optical Systems, Inc., Ann Arbor, MI, USA), equipped with a non-contact PhAT-probe. A 400 mW laser at 785 nm with a circular spot size of D = 6 mm was used. Working distance between probe and sample was 25 cm. The measured spectral range was 200–1890 cm^{-1}. Each spectrum was an average of 4 × 20 s accumulations, measured in triplicate, giving a total acquisition time of 320 s for each sample. The average of the three spectra were taken after fluorescence background subtraction.

To account for possible heterogeneity of the samples, apples were spun around their own axis during spectral collection. Each sample was first measured with skin. The apples were then peeled with a vegetable peeler and measured again in the same way. After that, the apple was cut in a half for starch index determination and the other half was used to obtain juice with a juice maker (Philips HR1866/00). The peduncle was removed, and the remains of the peeled apple were then juiced. The juice was frozen at −18 °C after measuring SSC for further analysis. The time for the entire procedure was less than 20 min per apple, avoiding oxidation of samples.

2.4. Multivariate data analysis

The fluorescence background in the raw Raman spectra was removed for the spectral range we used for analysis; from 300–1500 cm^{-1}. Polynomial fitting was applied to fit the background, using a polynomial degree of 6 and using in-house Matlab scripts (R2007b, The MathWorks, Inc., Natick, MA, USA). The method is based on a well-established algorithm [21,27,31].

To explore the spectral variation between and within the apple varieties, principal component analysis (PCA) was used [32]. Partial least-squares regression (PLSR) [33] was used to obtain calibration models between Raman spectra and the quality features. Full cross-validation was used to determine the number of components to use in the calibration models and a test set was used for validation. In the case of 'Aroma' samples, 70 samples were used for calibration and 35 samples for validation (randomly selected along weeks), and in the case of 'Elstar' samples, 63 were used as calibration set and 27 as test set. Calibration and validation analyses were performed using The Unscrambler version 6.11 (CAMO Software AS, Oslo, Norway). In addition, results were compared for non-normalized spectra and spectra normalized with standard normal variate (SNV) [34]. The performance of the models was evaluated using the following statistic parameters: determination coefficient (R^2), root mean square error of prediction (RMSEP), and relative error of prediction (REP). This last parameter was calculated by dividing RMSEP by the mean value of each parameter and expressed in percentage.

3. Results and discussion

3.1. Evolution of quality parameters during ripening

The overall development and variability of quality parameters over time is shown in Fig. 1. For starch (Fig. 1A), the content was higher in 'Elstar' (lower indices) than 'Aroma' at all harvesting days, with a clear decrease (higher indices) over time. The degradation was more pronounced for 'Aroma' than for 'Elstar'. Moreover, there were high standard deviations per day, indicating huge variability of samples within each sampling point. SSC mainly increased with time (Fig. 1B), but mostly towards the end of the sampling period. The SSC of the 'Elstar' samples was also higher than 'Aroma' at all time points. As expected, the development of SSC was quite like the trend observed for total sugars (Fig. 3F).

In the case of glucose (Fig. 1C), mean values for both varieties were at the same level and did not change much during the ripening process. For 'Aroma' apples there was a small increase of glucose content at the end of the sampling period. The sucrose content (Fig. 1E) on the other hand, increased steadily with time in both varieties, being higher for 'Elstar'. Regarding fructose (Fig. 1D), higher mean values were found for 'Aroma', although the values were similar along the ripening process. As mentioned before, in all cases, the standard deviations at each harvesting point were high, which indicates high intra-day variability of the samples.

The Pearson's correlations between the different quality parameters are presented in Fig. 2. For 'Aroma' there was a high and positive correlation between total sugars and SSC ($p < 0.05$). In addition, sucrose correlated highly with total sugars, and a positive correlation between glucose and fructose was obtained. The other correlations for Aroma were not significant ($p > 0.05$). This was the case for the correlations between e.g., SSC and glucose and between sucrose and fructose. For the 'Elstar' apples, similar correlations were obtained. A high positive correlation between sucrose and SSC was observed. In addition, significant correlations between total sugars and SSC and between fructose and glucose were found. These results are in accordance with earlier findings [27].

3.2. Spectral information

Firstly, Raman spectra were background corrected as described in section 2.4. The fluorescence background in the raw Raman spectra was removed for the spectral range that was used for analysis: 300–1500 cm^{-1}. Examples of raw and corrected spectra are presented in the Fig. S1.

Background corrected and normalized Raman spectra of all apples with and without skin are presented in Fig. 3. The spectra are colored according to the starch index obtained by the iodine staining (1 = high starch content and 10 = low starch content). The Raman spectra are rich in bands and information, and for both varieties, samples with skin (Fig. 3A and C) and without skin (Fig. 3B and D) were quite similar in shape and main bands. The most intense bands attributed to sugars are clearly visible at 420 (glucose and fructose), 629 (fructose), 835

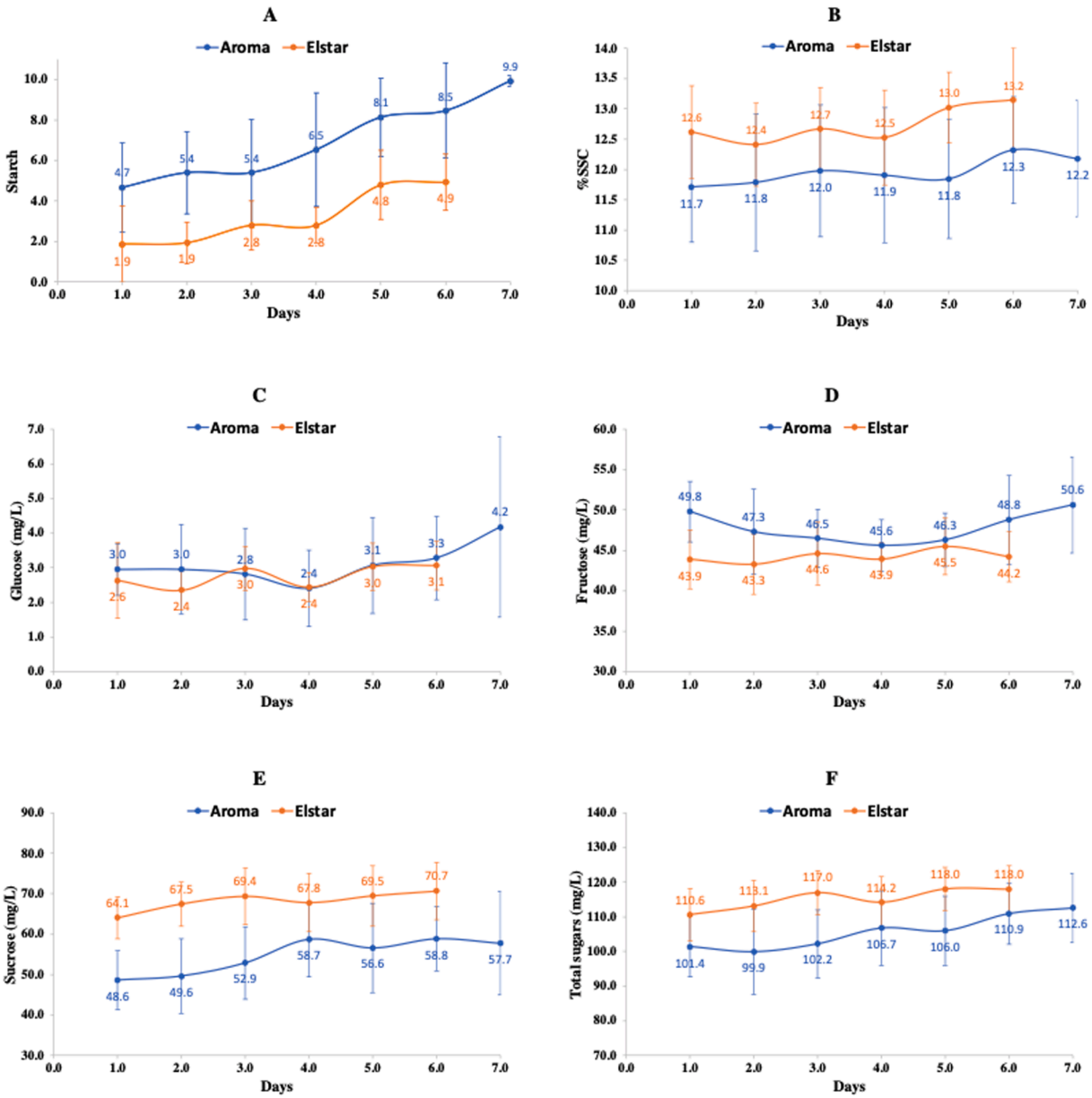

Fig. 1. Evolution of quality parameters of Aroma and Elstar over time: Starch index (A), Soluble Solids Content (SSC) (%) (B), glucose (mg/L) (C), fructose (mg/L) (D), sucrose (mg/L) (E) and total sugars (mg/L) (F).

(sucrose), 1083 (fructose), 1264 (fructose) and 1459 (fructose and glucose) cm^{-1}. This is in accordance with our previous work [27]. Fructose related bands dominated the spectra, which indicates that this was the most abundant sugar in the samples. Bands observed around 478, 940, and 1128 cm^{-1} are attributed to starch [35,36]. These bands tended to vary in intensity according to starch indices measured by the iodine method. Some samples with high intensity sugar bands had correspondingly low intensity starch bands. For the 'Elstar' apples, the starch content was visually clearer in the spectra compared to the 'Aroma' apples.

3.3. Principal component analysis (PCA)

PCA was applied to study the overall variation in the Raman spectra. For apples both with and without skin, the first principal components (PC1) separated the two varieties (Fig. 4A and C). The loadings for PC1 (Fig. 4B and D) revealed that the main Raman bands affecting the separation were 478, 940 and 1128 cm^{-1} associated with starch. Scores for PC1 were mainly positive for 'Elstar', indicating higher starch content. This is in accordance with the visual inspection of the spectra in Fig. 3. Also, there were some negative loadings in this component, which were more intense in the case of samples without skin. These bands at i.e., 420 and 628 cm^{-1}, can be attributed to fructose, and the loadings were of higher intensity for 'Aroma' apples. This is reasonable since the starch content was lower (higher starch indeces) in this variety compared to 'Elstar'.

PCA was also performed separately for each variety (apples with skin) and the score values are shown in Fig. 5. Samples in the plots were colored according to the weeks 1 to 3 (red) and weeks 4 to 6 (or 7). In both cases, there are indications that samples are distributed according to time since the first component was related to starch (PC loading 1 is showed in Fig. S2). This trend, however, is not clear, which most likely could be attributed to large chemical variations at each time point.

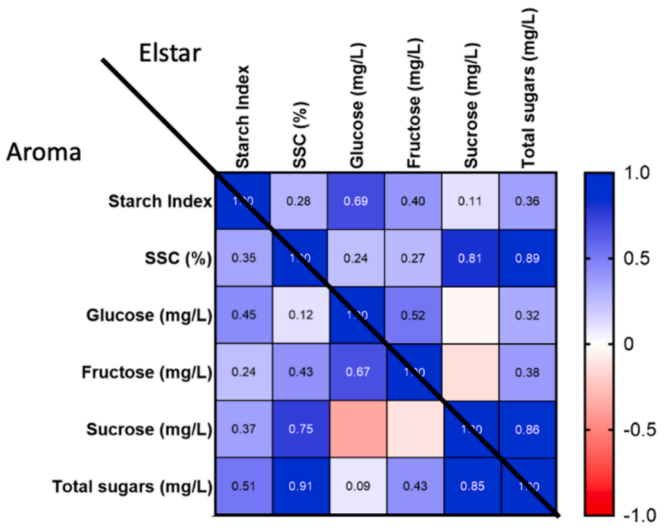

Fig. 2. Pearson's correlations between different chemical components in 'Aroma' (lower) and 'Elstar' apples (upper).

3.4. Calibration models

Baseline corrected and normalized spectra were used to obtain calibration models and predictions for all chemical reference parameters. The explained variance for each compound was used to select the optimal number of components in the models. In addition, the regression coefficients obtained were evaluated to assure that models were relying on meaningful spectral features. All results for calibration (cross validation) and test set validation are detailed in Table 2. In addition, the corresponding plots of predicted vs measured values are found in the Fig. S3 (Aroma) and Fig. S4 (Elstar), for models of apples with skin.

As expected, results were overall better for samples without skin, as observed previously [27]. The R^2 values for most models were higher for 'Aroma' due to larger spans in most reference values compared to 'Elstar', while the RMSEP (calibration and test set) values were quite similar.

A key parameter in the current study is the starch index since starch content is closely connected to fruit maturity. As seen in Table 2, for the 'Aroma' apples, with and without skin, 3 components were necessary for building the models, explaining 87 % and 81 % of the variance in starch index, respectively. For 'Elstar' with and without skin, 2 and 3 components were used for starch index models, explaining 63 and 67 % of the variance. Thus, for starch index we obtained better results for 'Aroma' than for 'Elstar'. The reason for this could be that the range of the starch index for 'Aroma' (from 2 to 10) was in the upper range compared to 'Elstar' (from 1 to 8). Similar results for the different varieties were obtained in the test set, being better for the 'Aroma' variety ($R^2 = 0.86$ and RMSEP=0.94). Regression coefficients for starch index models relied heavily on the starch band at 478 cm^{-1}, indicating a sound model. The regression coefficients for starch index are provided in Fig. 6 and for the other quality parameters are presented in Fig. S5. Here the main starch bands are negative since the starch index is inversely proportional to starch contents. REPs (%) were in the region 13–20 %, for 'Aroma', which can be considered as good results. In the case of 'Elstar', more samples would be necessary in order to expand the ranges of the data and to obtain better REPs, which are dependent on these values.

For SSC, the calibration results obtained were acceptable. For the 'Aroma' apples, R^2 was higher than 0.64, but for 'Elstar', R^2 was higher than 0.4. However, in both varieties the RMSEP for test set were lower than in other studies [27,37,38]. If the plots of predicted versus measured values are observed, the influence of the different ranges of 'Aroma' and 'Elstar' can be seen (Figs. S3 and S4). In addition, the REPs were lower than 6 %, which can be considered as a feasible result. The same Raman bands were emphasized in the regression coefficients for both varieties (Fig. S5A). A higher number of components were needed in these models compared with a recent study [27], which might be due to a larger variation in starch in the present study.

In the case of fructose, calibration models were obtained with R^2 above 0.41. However, when relative content of fructose was used as

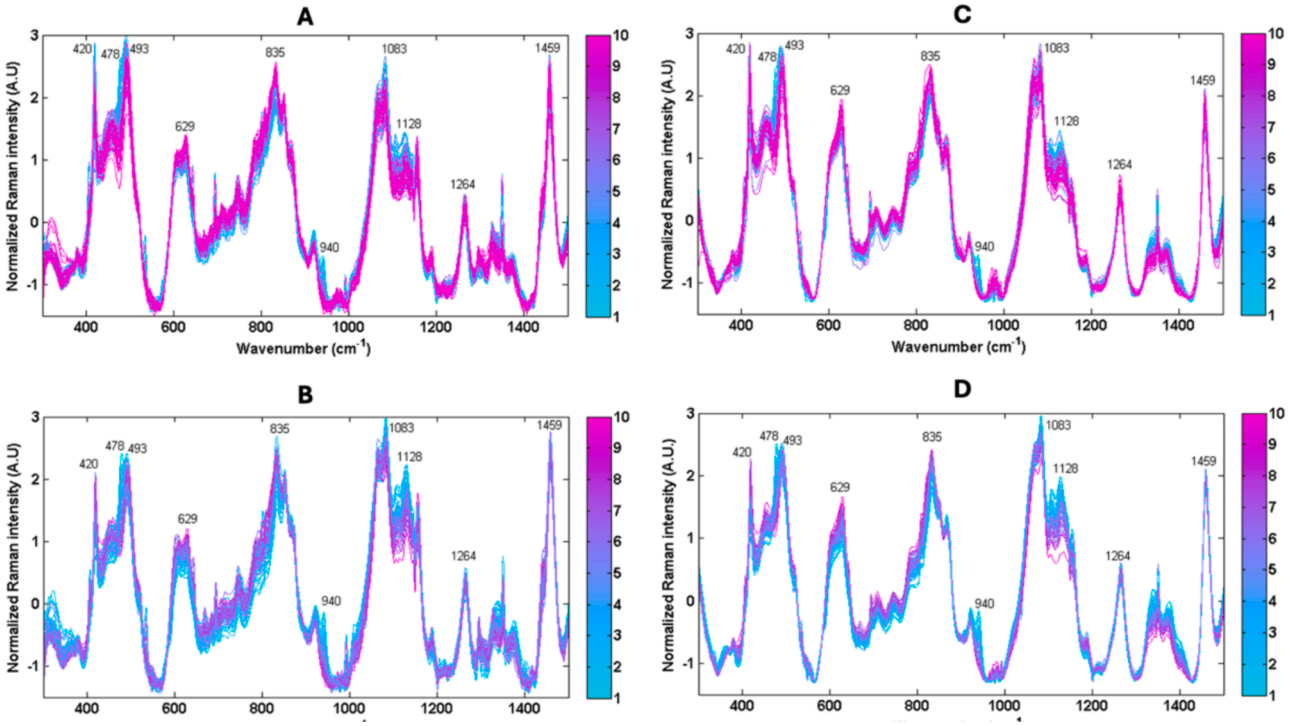

Fig. 3. Normalized Raman spectra of all samples: 'Aroma' apples with skin (A) and without skin (B); and 'Elstar' apples with skin (C) and without skin (D). The spectra are colored according to the starch index obtained by iodine staining (1 = high starch content and 10 = low starch content).

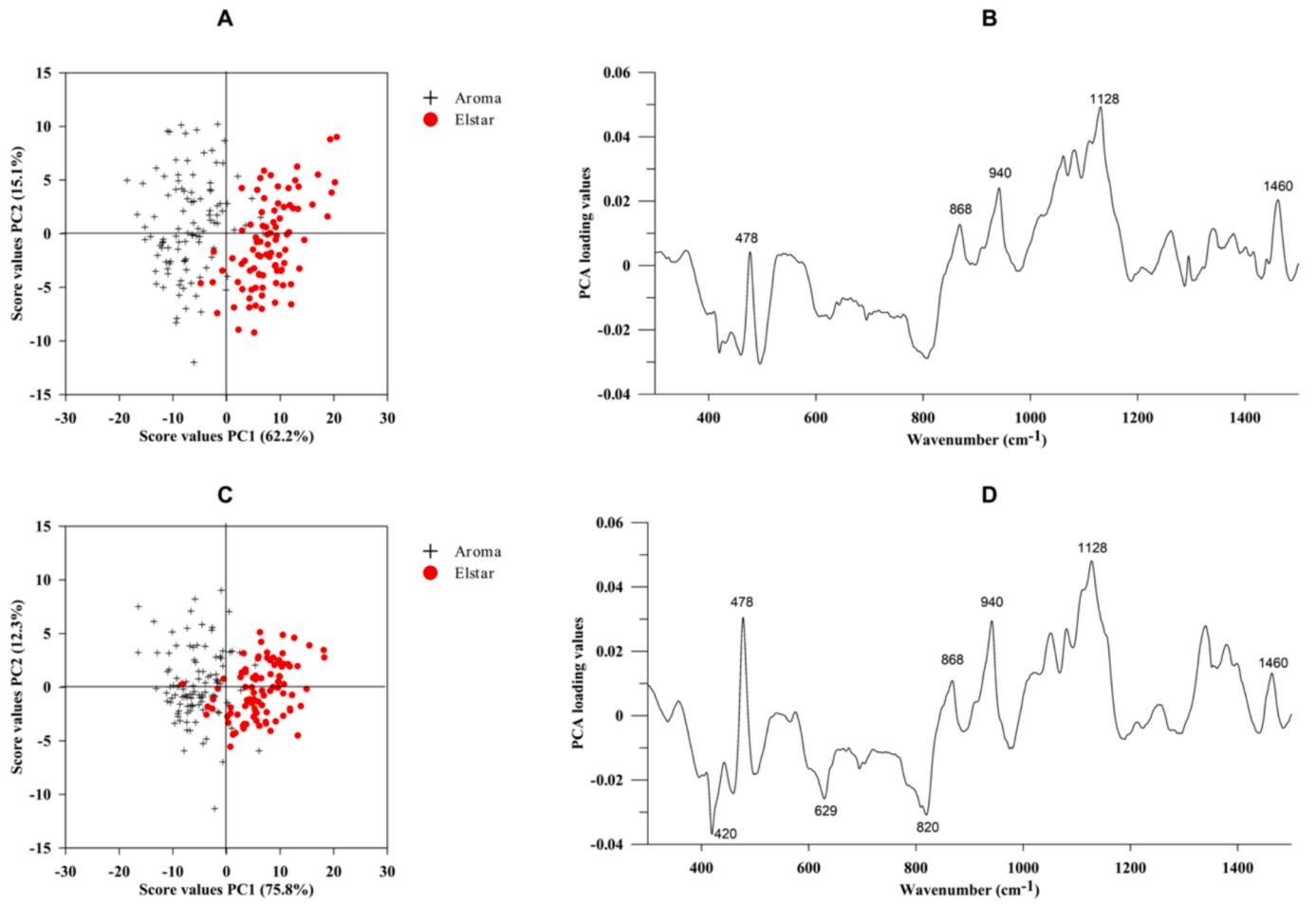

Fig. 4. Score values (A and C) for PC1 and PC2 and loadings for PC1 (B and D) obtained from PCA of Raman spectra from apples with skin (A and B) and without skin (C and D).

reference (i.e., as percentage of total sugars), the values for R^2 increased to 0.84 or more, obtaining values of RMSEP lower than 2.5 % in all cases. As observed in the regression coefficients of Fig. S5G, the main variables affecting these models were quite similar for both varieties and appeared at 629, 1264 and 1459 cm^1. These Raman shifts are associated with fructose [27]. Sucrose did also affect the model with a negative peak in the coefficients at 835 cm^{-1}. Similar improvements of model performance with relative contents instead of absolute contents were also seen for the sucrose models.

The poorest results in this study were obtained for glucose, which was expected, due to the low concentrations in the samples (1.3–8.2 mg/L for 'Aroma' and 1.6–4.7 mg/L for 'Elstar'). In all calibrations, the RMSEP (CV) was lower than 0.58 mg/L and the REP (%) was lower than 27 %. In the case of test set validation, similar results were obtained (Table 2). When these models were compared with models obtained for relative glucose contents the results did not improve much. The corresponding regression coefficients showed influent variables at 422, 629, 1064, 1264 and 1459 cm^{-1}, most of which corresponded to fructose instead of glucose. These sugars correlated positively (Fig. 2), which might explain this result.

In the current study, both normalized and non-normalized Raman spectra were used for the calibration studies. For most models, normalized spectra were preferred, but for some of the SSC and starch models, the non-normalized Raman spectra provided better results (data not shown). The reason behind this result is open for discussion, but one hypothesis is that when modelling bulk or gross components (like e.g., starch index or SSC), the non-normalized spectra are needed to capture the relevant spectral information, but for minor components like individual sugars, normalization is needed to standardize spectra and remove non-relevant variation [22]. A related and intriguing finding is that for all individual sugars, relative concentrations are better modelled than absolute values. An exception to this finding was glucose, where there was no difference between the two approaches. Apparently, the Raman signatures were better related to the relative contents of the sugars, which could be attributed to the overall scattering efficiencies of the components present. This is clearly a result that should be kept in mind in future studies. Similar results have been obtained for other food matrices, for instance related to expressing absolute and relative contents of fatty acids in fish muscles [39].

Overall, the present calibration and validation results show the feasibility of using Raman spectroscopy to predict chemistry of apples during ripening. Although a range of parameters could be predicted with low estimation errors, other parameters show correlations that are too low to be of practical use. For these parameters, increasing the number of samples and also expanding the ranges of the parameters would be one way to potentially improve calibration performances. It is therefore encouraging to see that most calibrations are built on chemically logic Raman features (based on the regression coefficients). Finally, the use of calibrations based on one variety to estimate quality parameters in the other variety was attempted but was not successful due to the differences in varieties. However, when all samples were modelled together by the use of cross-validation, the results were acceptable (data not shown), but a higher number of components was required due to increased complexity of the combined data.

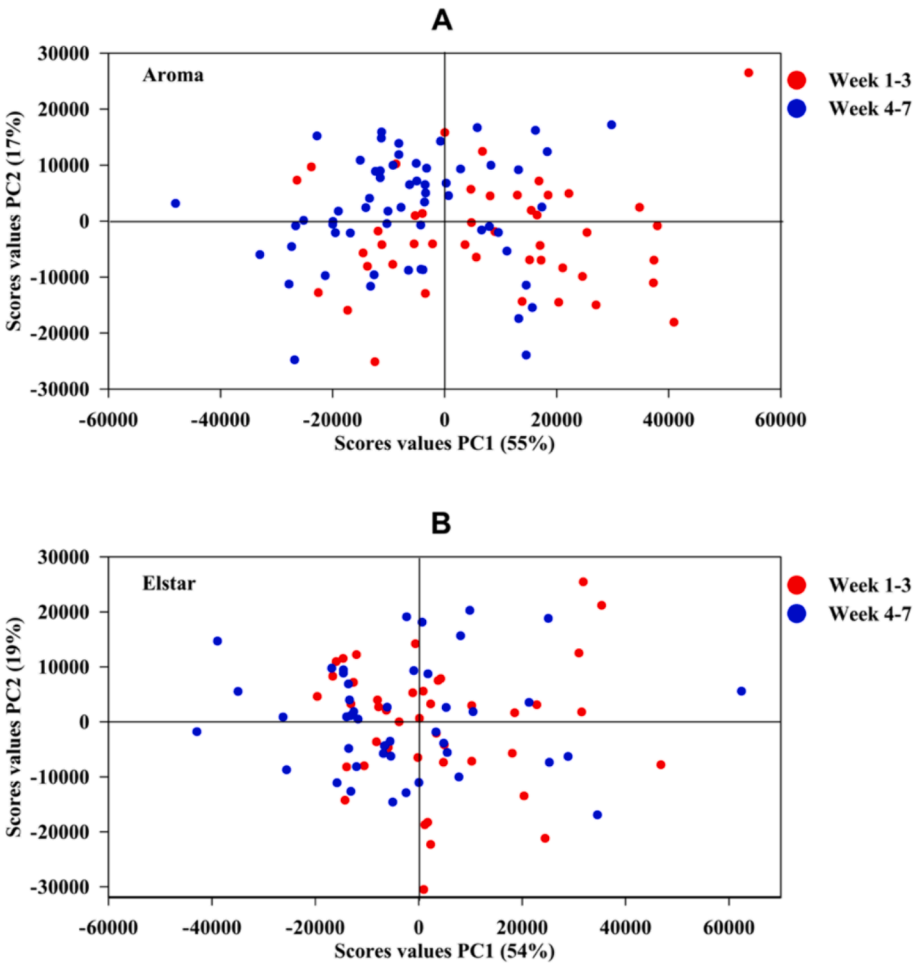

Fig. 5. Score values obtained from PCA of Raman spectra from apples with skin: Aroma (A) and Elstar (B).

3.5. General discussion

To our knowledge, this is the first time Raman spectroscopy has been used to measure starch index in whole apples. The reference method for the evaluation of starch index is an uncertain analysis based on destructive analysis and personal assessment. Thus, the starch index models could most likely be improved by using a more extensive laboratory analysis for obtaining results of lower uncertainties. There might also be a sampling mismatch between the Raman spectra collected from the outer part of the apple and the iodine method. For apples with high starch contents, the changes in the starch index range from e.g. 1–5, can be difficult to detect with Raman, since the changes apparently occur in the inner part of the apple, out of range of the Raman probe. When degradation of starch has reached a higher index level (5–10), indicating more ripe apples, the degradation of starch occurs more in the outer part of the apple and the changes in concentration can be detectable with the Raman probe. This means that the current Raman probe might be sensitive in the 5–10 range, but less sensitive in the 1–5 range. On the contrary, other authors observed a higher starch concentration in the outer part of the apple flesh and lower around the core [40]. They also reported that the starch degradation started simultaneously in the whole apple, but with higher speed in the outer part of the apple. If this is the case, then Raman spectroscopy might be highly representative for non-destructive assessment of the ripening process and starch degradation in apples.

It is worth reminding that NIR spectroscopy is not very well suited for starch index determination in apples. Other authors demonstrated that since much of the starch converts to sugars during ripening, NIRS is not able to distinguish between insoluble and soluble carbohydrates, making it difficult to obtain accurate predictions. An inability to discriminate between starch and soluble sugars could explain the lack of studies of starch with NIRS along the ripening period [41]. A few studies have reported somewhat promising results with NIRS for determining starch index. McGlone et al. used VIS/NIRS to estimate different quality indeces in 'Royal Gala' apples. They obtained a RMSEP of 0.95 for the starch pattern index [7]. Another example was developed by Bertone et al., they evaluated the ripening of red apples ('Scarlet') using NIR spectroscopy. In the determination of starch index, they obtained a RMSEP in the test set of 1.7, which was higher that the results obtained in this work [38]. Pissard et al. also evaluated a handheld ultra-compact NIR spectrometer for starch index determination [8] and obtained a RMSEP of 0.84. All results studies are comparable to those obtain in this work.

Presently, Raman spectroscopy has some practical drawbacks compared to for instance NIR spectroscopy. The need for rather long exposure times is a limitation with respect to high throughput screening in field or in the lab. This exposure time can however be shortened with optimal instrumentation. It has been shown that Raman can be used to scan e.g. salmon fillets at high speed and obtain spectra with sufficient SNR in 1–2 sec [24]. Another challenge with Raman is the sensitivity to ambient light, due to the rather low Raman signals. This is less of a problem indoors, where room light can be selected to not interfere with the Raman spectrum, but for field measurements, the sunlight will introduce noise. The same challenge exists for NIR spectroscopy and has been solved by using contact measurements with a light-insulating cover. The same solution can be used for Raman measurements.

Table 2
Results obtained for the different models assayed and the test set.

AROMA	SKIN							WITHOUT SKIN						
	Calibration set				Test set			Calibration set				Test set		
	Comp.	$RMSEP_{CV}$	REP_{CV} (%)	R^2_{CV}	RMSEP	REP (%)	R^2_P	Comp.	$RMSEP_{CV}$	REP_{CV} (%)	R^2_{CV}	RMSEP	REP (%)	R^2_P
SSC (%)	4	0.60	5.1	0.64	0.64	4.9	0.62	4	0.62	5.2	0.64	0.61	5.0	0.65
Starch index	3	1	15	0.86	0.94	13	0.86	3	1.3	20	0.81	1.1	16	0.85
Total sugars (mg/L)	5	6.0	5.7	0.72	6.6	5.7	0.61	4	5.5	5.3	0.76	5.7	5.3	0.69
Glucose (mg/L)	4	0.73	24	0.81	0.97	29	0.46	7	0.54	18	0.90	0.66	20	0.73
Glucose (%)	4	0.78	27	0.78	1.0	33	0.38	7	0.52	18	0.90	0.69	23	0.71
Fructose (mg/L)	4	3.2	6.8	0.50	3.5	7.2	0.61	5	2.4	5.1	0.72	2.9	5.9	0.71
Fructose (%)	6	2.0	4.4	0.84	2.5	5.5	0.75	3	1.8	3.9	0.87	1.8	4.0	0.86
Sucrose (mg/L)	6	4.6	8.5	0.81	5.5	9.7	0.66	3	4.6	8.5	0.81	4.1	7.3	0.81
Sucrose (%)	6	2.4	4.7	0.85	3.2	6.2	0.70	3	2.3	4.5	0.87	2.2	4.9	0.85
ELSTAR	Calibration set				Test set			Calibration set				Test set		
	Comp.	$RMSEP_{CV}$	REP_{CV} (%)	R^2_{CV}	RMSEP	REP (%)	R^2_P	Comp.	$RMSEP_{CV}$	REP_{CV} (%)	R^2_{CV}	RMSEP	REP (%)	R^2_P
SSC (%)	4	0.67	5.3	0.29	0.59	4.7	0.40	6	0.52	4.1	0.56	0.57	4.5	0.39
Starch index	2	1.2	45	0.63	1.0	43	0.69	3	1.0	37	0.67	0.92	7.2	0.62
Total sugars (mg/L)	4	5.7	5.0	0.38	5.6	5.0	0.37	4	5.0	4.4	0.57	5.3	4.7	0.49
Glucose	4	0.58	22	0.51	0.53	20	0.43	4	0.49	18	0.70	0.32	12	0.79
Glucose (%)	6	0.44	19	0.54	0.41	18	0.54	5	0.36	16	0.72	0.26	11	0.85
Fructose (mg/L)	3	2.6	5.9	0.41	2.4	5.5	0.35	5	2.0	4.5	0.69	1.7	3.9	0.74
Fructose (%)	6	1.7	4.4	0.70	1.2	3.2	0.83	5	1.0	2.9	0.86	0.68	1.8	0.95
Sucrose (mg/L)	2	4.4	6.5	0.57	4.7	7.0	0.53	5	4.0	5.9	0.62	3.3	4.9	0.75
Sucrose (%)	7	1.8	3.0	0.72	1.6	2.7	0.76	5	1.2	2.0	0.84	0.81	1.4	0.94

Comp.: components; CV: cross-validation; RMSEP: root mean square error of prediction; REP: relative error of prediction.

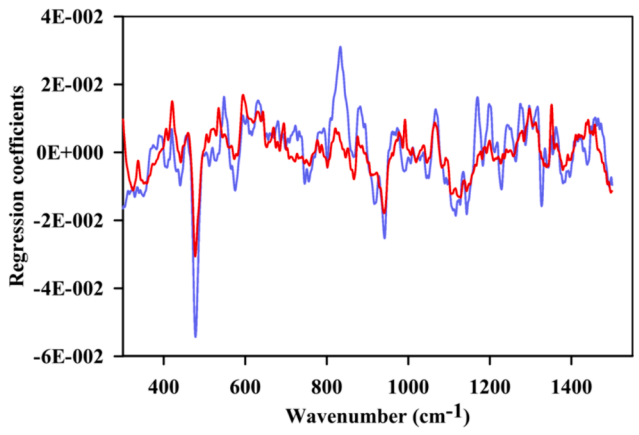

Fig. 6. Regression coefficients for starch index models obtained for apples with skin ('Aroma' in blue, 'Elstar' in red).

The importance of starch determination is crucial in apple handling. For example, apples with high starch content (starch index range 3–5) are most likely to be harvested for long-term storage, while apples with lower content (6–10) are recommended for the fresh market [42]. Hence, the use of non-destructive analysis might be a good solution in a packing and sorting line to e.g. ensure the same ripening stages in a 6-pack of apples. Raman could, in the future, be used by the grower (or robots) to monitor or measure the ripening process on the fruit trees and point out which apples to harvest at the right time, depending on the use (short- or long-term storage). Many places the farmers harvest several times because the ripening process is different within the same crop in the tree. This is a costly time in the production, so to do this more efficient and with lower waste, could increase the overall value of apples.

4. Conclusions

This study evaluated the potential of Raman spectroscopy for monitoring typical chemical parameters related to ripeness in two Norwegian grown apple varieties. The Raman spectra expressed distinct vibrational bands for starch and the sugars sucrose, glucose and fructose and predictive performances were good, except for glucose. Better results for individual sugars were obtained when contents were expressed in relative values and spectra were normalized. New to this study was the use of Raman spectroscopy to measure starch index in apples, the first to our knowledge. The promising results suggest that Raman might be a future tool in harvest management of apples.

CRediT authorship contribution statement

Olga Monago-Maraña: Writing – review & editing, Writing – original draft, Methodology, Investigation, Formal analysis, Conceptualization. **Jens Petter Wold:** Writing – review & editing, Writing – original draft, Supervision, Methodology, Funding acquisition, Conceptualization. **Siv Fagertun Remberg:** Writing – review & editing, Methodology, Conceptualization. **Karen Wahlstrøm Sanden:** Writing – review & editing, Methodology, Investigation. **Nils Kristian Afseth:** Writing – review & editing, Writing – original draft, Supervision, Methodology, Funding acquisition, Conceptualization.

Declaration of competing interest

The authors declare that they have no known competing financial interests or personal relationships that could have appeared to influence the work reported in this paper.

Data availability

Data will be made available on request.

Acknowledgements

Olga Monago Maraña thanks to the Fundación Ramón Areces for a postdoctoral fellowship for studies abroad in the field of Life and Matter Sciences (XXXI edition of grants, 2019/2020) to support her post-doctoral studies at Nofima, Ås, Norway. The work was funded by the Norwegian Agricultural Food Research Foundation through the projects Precision Food Production (NRC project number 314111) and SusHealth (NRC project number 314599). Funding from the Research Council of Norway through the project "SFI Digital Food Quality" (no. 309259) is also greatly acknowledged.

Appendix A. Supplementary data

Supplementary data to this article can be found online at https://doi.org/10.1016/j.saa.2024.124903.

References

[1] H. Zhou, X. Wang, W. Au, H. Kang, C. Chen, Intelligent robots for fruit harvesting: recent developments and future challenges, Precis. Agric. 23 (2022) 1856–1907, https://doi.org/10.1007/s11119-022-09913-3.
[2] R. Van Beers, B. Aernouts, L. León Gutiérrez, C. Erkinbaev, K. Rutten, A. Schenk, B. Nicolaï, W. Saeys, Optimal illumination-detection distance and detector size for predicting Braeburn apple maturity from Vis/NIR laser reflectance measurements, Food Bioproc. Tech. 8 (2015) 2123–2136, https://doi.org/10.1007/s11947-015-1562-4.
[3] F.R. Harker, F.A. Gunson, S.R. Jaeger, The case for fruit quality: An interpretive review of consumer attitudes, and preferences for apples, Postharvest Biol. Technol. 28 (2003) 333–347, https://doi.org/10.1016/S0925-5214(02)00215-6.
[4] Y. Guan, C. Peace, D. Rudell, S. Verma, K. Evans, QTLs detected for individual sugars and soluble solids content in apple, Mol. Breed. 35 (2015), https://doi.org/10.1007/s11032-015-0334-1.
[5] R. Pourdarbani, S. Sabzi, D. Kalantari, J.I. Arribas, Non-destructive visible and short-wave near-infrared spectroscopic data estimation of various physicochemical properties of Fuji apple (Malus pumila) fruits at different maturation stages, Chemom. Intel. Lab. Syst. 206 (2020) 104147, https://doi.org/10.1016/j.chemolab.2020.104147.
[6] R. Pourdarbani, S. Sabzi, D. Kalantari, J. Paliwal, B. Benmouna, G. García-Mateos, J.M. Molina-Martínez, Estimation of different ripening stages of Fuji apples using image processing and spectroscopy based on the majority voting method, Comput. Electron. Agric. 176 (2020) 105643, https://doi.org/10.1016/j.compag.2020.105643.
[7] V.A. Mcglone, R.B. Jordan, P.J. Martinsen, Vis/NIR estimation at harvest of pre- and post-storage quality indices for "Royal Gala" apple, 2002. www.elsevier.com/locate/postharvbio.
[8] A. Pissard, E.J.N. Marques, P. Dardenne, M. Lateur, C. Pasquini, M.F. Pimentel, J.A. Fernández Pierna, V. Baeten, Evaluation of a handheld ultra-compact NIR spectrometer for rapid and non-destructive determination of apple fruit quality, Postharvest. Biol. Technol. 172 (2021). DOI: 10.1016/j.postharvbio.2020.111375.
[9] K.B. Walsh, J. Blasco, M. Zude-Sasse, X. Sun, Visible-NIR 'point' spectroscopy in postharvest fruit and vegetable assessment: The science behind three decades of commercial use, Postharvest. Biol. Technol. 168 (2020), https://doi.org/10.1016/j.postharvbio.2020.111246.
[10] O. Abbas, A. Pissard, V. Baeten, Near-infrared, mid-infrared, and Raman spectroscopy, in: Chemical Analysis of Food, Elsevier, 2020, pp. 77–134, https://doi.org/10.1016/b978-0-12-813266-1.00003-6.
[11] Y. Sun, H. Tang, X. Zou, G. Meng, N. Wu, Raman spectroscopy for food quality assurance and safety monitoring: a review, Curr. Opin. Food Sci. 47 (2022) 100910, https://doi.org/10.1016/j.cofs.2022.100910.
[12] E. Wiercigroch, E. Szafraniec, K. Czamara, M.Z. Pacia, K. Majzner, K. Kochan, A. Kaczor, M. Baranska, K. Malek, Raman and infrared spectroscopy of carbohydrates: A review, Spectrochim. Acta A Mol. Biomol. Spectrosc. 185 (2017) 317–335, https://doi.org/10.1016/j.saa.2017.05.045.
[13] B. Özbalci, I.H. Boyaci, A. Topcu, C. Kadilar, U. Tamer, Rapid analysis of sugars in honey by processing Raman spectrum using chemometric methods and artificial neural networks, Food Chem. 136 (2013) 1444–1452, https://doi.org/10.1016/j.foodchem.2012.09.064.
[14] K. Ilaslan, I.H. Boyaci, A. Topcu, Rapid analysis of glucose, fructose and sucrose contents of commercial soft drinks using Raman spectroscopy, Food Control 48 (2015) 56–61, https://doi.org/10.1016/j.foodcont.2014.01.001.
[15] M.R. Almeida, R.S. Alves, L.B.L.R. Nascimbem, R. Stephani, R.J. Poppi, L.F.C. De Oliveira, Determination of amylose content in starch using Raman spectroscopy and multivariate calibration analysis, Anal. Bioanal. Chem. 397 (2010) 2693–2701, https://doi.org/10.1007/s00216-010-3566-2.
[16] Y. Ji, Y. He, Y. Cui, T. Wang, Y. Wang, Y. Li, W.E. Huang, J. Xu, Raman spectroscopy provides a rapid, non-invasive method for quantification of starch in live, unicellular microalgae, 2014. DOI: 10.1002/biot.201400165.Submitted.
[17] K.A. Esmonde-White, M. Cuellar, C. Uerpmann, B. Lenain, I.R. Lewis, Raman spectroscopy as a process analytical technology for pharmaceutical manufacturing and bioprocessing, Anal. Bioanal. Chem. 409 (2017) 637–649, https://doi.org/10.1007/s00216-016-9824-1.
[18] P. Matousek, M.D. Morris, N. Everall, I.P. Clark, M. Towrie, E. Draper, A. Goodship, A.W. Parker, Numerical simulations of subsurface probing in diffusely scattering media using spatially offset Raman spectroscopy, Appl. Spectrosc. 59 (2005) 1485–1492, https://doi.org/10.1366/000370205775142548.
[19] J. Qin, K. Chao, M.S. Kim, Investigation of Raman chemical imaging for detection of lycopene changes in tomatoes during postharvest ripening, J. Food Eng. 107 (2011) 277–288, https://doi.org/10.1016/j.jfoodeng.2011.07.021.
[20] J. Qin, K. Chao, M.S. Kim, Nondestructive evaluation of internal maturity of tomatoes using spatially offset Raman spectroscopy, Postharvest Biol. Technol. 71 (2012) 21–31, https://doi.org/10.1016/j.postharvbio.2012.04.008.
[21] O. Monago-Maraña, J.P. Wold, R. Rødbotten, K.R. Dankel, N.K. Afseth, Raman, near-infrared and fluorescence spectroscopy for determination of collagen content in ground meat and poultry by-products, Lwt 140 (2021), https://doi.org/10.1016/j.lwt.2020.110592.
[22] P.V. Andersen, J.P. Wold, N.K. Afseth, Assessment of bulk composition of heterogeneous food matrices using Raman spectroscopy, Appl. Spectrosc. 75 (2021) 1278–1287, https://doi.org/10.1177/00037028211006150.
[23] J.D. Landry, P.J. Torley, E.W. Blanch, Quantitation of carotenoids and fatty acids from Atlantic salmon using a portable Raman device, Analyst 147 (2022) 4379–4388, https://doi.org/10.1039/D2AN01140A.
[24] T.A. Lintvedt, P.V. Andersen, N.K. Afseth, K. Heia, S.K. Lindberg, J.P. Wold, Raman spectroscopy and NIR hyperspectral imaging for in-line estimation of fatty acid features in salmon fillets, Talanta 254 (2023) 124113, https://doi.org/10.1016/j.talanta.2022.124113.
[25] T.A. Lintvedt, P.V. Andersen, N.K. Afseth, J.P. Wold, In-line Raman spectroscopy for characterization of an industrial poultry raw material stream, Talanta 266 (2024), https://doi.org/10.1016/j.talanta.2023.125079.
[26] P.V. Andersen, N.K. Afseth, K. Aaby, M.Ø. Gaarder, S.F. Remberg, J.P. Wold, Prediction of chemical and sensory properties in strawberries using Raman spectroscopy, Postharvest Biol. Technol. 201 (2023), https://doi.org/10.1016/j.postharvbio.2023.112370.
[27] O. Monago-Maraña, N.K. Afseth, S.H. Knutsen, S.G. Wubshet, J.P. Wold, Quantification of soluble solids and individual sugars in apples by Raman spectroscopy: A feasibility study, Postharvest Biol. Technol. 180 (2021), https://doi.org/10.1016/j.postharvbio.2021.111620.
[28] T. Helgerud, S.H. Knutsen, N.K. Afseth, K.F. Stene, E.O. Rukke, S. Ballance, Evaluation of hand-held instruments for representative determination of glucose in potatoes, Potato Res. 59 (2016) 99–112, https://doi.org/10.1007/s11540-015-9310-8.
[29] M.K. Ernst, G. Matitschka, N.J. Chatterton, P.A. Harrison, A quantitative histochemical procedure for measurement of starch in apple fruits, 1999.
[30] J.P. Quast, Fruchtentwicklung und Fruchtreife. I. Ernteterminbestimmung Bei Frühäpfeln, Obstbau 8 (1991) 391–394.
[31] C.A. Lieber, A. Mahadevan-Jansen, Automated method for subtraction of fluorescence from biological Raman spectra, Appl. Spectrosc. 57 (2003) 1363–1367.
[32] S. Wold, K.I.M. Esbensen, P. Geladi, Principal component analysis, Chemom. Intel. Lab. Syst. 2 (1987) 37–52.
[33] H. Martens, T. Naes, Multivariate Calibration, Wiley, New York, 1989.
[34] R.J. Barnes, M.S. Dhanoa, S.J. Lister, Standard Normal Variate Transformation and De-trending of Near-Infrared Diffuse Reflectance Spectra, 1989.
[35] V.G. Kelis Cardoso, R.J. Poppi, Cleaner and faster method to detect adulteration in cassava starch using Raman spectroscopy and one-class support vector machine, Food Control 125 (2021) 107917.
[36] J. Kniese, A.M. Race, H. Schmidt, Classification of cereal flour species using Raman spectroscopy in combination with spectra quality control and multivariate statistical analysis, J. Cereal Sci. 101 (2021) 103299.
[37] Y. Zhang, J.F. Nock, Y. Al Shoffe, C.B. Watkins, Non-destructive prediction of soluble solids and dry matter contents in eight apple cultivars using near-infrared spectroscopy, Postharvest Biol. Technol. 151 (2019) 111–118. DOI: 10.1016/j.postharvbio.2019.01.009.
[38] E. Bertone, A. Venturello, R. Leardi, F. Geobaldo, Prediction of the optimum harvest time of "Scarlet" apples using DR-UV-Vis and NIR spectroscopy, Postharvest Biol. Technol. 69 (2012) 15–23, https://doi.org/10.1016/j.postharvbio.2012.02.009.
[39] N.K. Afseth, K. Dankel, P.V. Andersen, G.F. Difford, S.S. Horn, A. Sonesson, B. Hillestad, J.P. Wold, E. Tengstrand, Raman and near infrared spectroscopy for quantification of fatty acids in muscle tissue—A Salmon case study, Foods 11 (2022), https://doi.org/10.3390/foods11070962.
[40] P. Brookfield, P. Murphy, R. Harker, E. Macrae, Starch degradation and starch pattern indices; interpretation and relationship to maturity, Postharvest Biol. Technol. (1997).
[41] X. Luo, Z. Ye, H. Xu, D. Zhang, S. Bai, Y. Ying, Robustness improvement of NIR-based determination of soluble solids in apple fruit by local calibration, Postharvest Biol. Technol. 139 (2018) 82–90.
[42] M. Małachowska, K. Tomala, Apple quality during shelf-life after long-term storage and simulated transport, Agriculture 13 (2023) 2045, https://doi.org/10.3390/agriculture13112045.